


RESEARCH

Open Access



# Adaptive coding and modulation using imperfect CSI in cognitive BIC-OFDM systems

Jeroen Van Hecke<sup>1\*</sup> , Paolo Del Fiorentino<sup>2</sup>, Riccardo Andreotti<sup>2</sup>, Vincenzo Lottici<sup>2</sup>, Filippo Giannetti<sup>2</sup>, Luc Vandendorpe<sup>3</sup> and Marc Moeneclaey<sup>1</sup>

## Abstract

This work investigates adaptive coding and modulation (ACM) algorithms under the realistic assumption that the available channel state information (CSI) at the transmitter is imperfect due to estimation errors and/or feedback delays. First, we introduce an optimal performance metric for the secondary user (SU) bit-interleaved coded orthogonal frequency division multiplexing (BIC-OFDM) system, called the expected goodput (EGP). By using an accurate modeling approximation, we succeed in deriving a tractable and very accurate approximation for the EGP. This approximate EGP (AEGP) is then used for the derivation of several ACM algorithms which optimize the code rate and bit and energy allocation under a constraint on the interference caused to the PU network. In the numerical results, we show that the AEGP is far more accurate than previous attempts to model the GP in the presence of imperfect CSI. Further, we verify that, in spite of the imperfect nature of the available CSI, the derived ACM algorithms significantly increase the goodput of the SU network, compared to a non-adaptive selection of the transmission parameters.

**Keywords:** Effective SNR mapping (ESM), Orthogonal frequency division multiplexing (OFDM), Adaptive coding and modulation (ACM), Imperfect channel state information, Goodput

## 1 Introduction

To meet the demand of high data rates and the increasing amount of traffic, the current and next generation of wireless networks need spectrally efficient solutions such as multicarrier orthogonal frequency division multiplexing (OFDM) transmission, efficient channel coding techniques in the form of bit interleaved coded modulation (BICM) [1], and adaptive coding and modulation (ACM) [2]. To further increase the spectral efficiency, the idea of cognitive radio (CR) [3, 4] has been proposed. This technique allows unlicensed or secondary users (SUs) to transmit over sections of spectrum owned by licensed or primary users (PUs), on the condition that the former do not harm the quality of service (QoS) of the latter.

If channel state information (CSI) is available at the transmitter, ACM can significantly improve the performance of the network by adapting the transmission parameters, such as energy and bit allocation per subcarrier, constellation size, and code rate, to the actual state

of the channel. However, in a wireless environment, the CSI at the transmitter, obtained from channel estimates fed back by the receiver, will be *imperfect*, due to channel estimation errors at the receiver and, in the case of a time-varying channel, the feedback delay on the return channel from the receiver to the transmitter. In [5], the authors show for a single user OFDM system that, even with CSI imperfections at the transmitter, the throughput of the system can be significantly increased by using adaptive modulation. The adaptation algorithms take the CSI imperfections into account, and their performance was shown to improve by having multiple estimates available at the transmitter. This means that, when multiple estimates are available, the network can tolerate larger channel estimation errors or longer delays, while still achieving an acceptable performance level. In [6], this scenario was extended to a multi-user OFDMA-system where the subcarriers are allocated to the user with the best signal-to-noise ratio (SNR) conditions and the number of bits per subcarrier are optimized by maximizing the average throughput. However, the results in [5, 6] were obtained for an uncoded OFDM system; this considerably simplifies the optimization problem (OP) because the

\*Correspondence: jeroen.vanhecke@ugent.be

<sup>1</sup>Ghent University, Department of Telecommunications and Information Processing, 9000 Ghent, Belgium

Full list of author information is available at the end of the article

probability of a bit error on a subcarrier only depends on the SNR of the considered subcarrier, but the results are of limited use in a practical scenario where channel coding is used.

In recent years, there have been several works [7–12] that studied resource allocation in cognitive underlay networks with imperfect CSI. However, these works used a more theoretic performance metric like the capacity metric or SNR and did not consider the difficult problem of implementing ACM in a practical coded multi-carrier transmission system. Because the bits are coded and the channel is frequency-selective, the throughput of the network depends upon a complicated function of the SNRs of all the subcarriers which are used for the transmission. A technique which allows to simplify the analytical expression for the performance metric is effective SNR mapping (ESM) [13]. This technique transforms the vector of subcarrier SNRs, which affect the codeword, into a scalar SNR. This effective SNR is the operating point at which an equivalent coded system, which uses the same modulation and coding scheme, operating over an additive white Gaussian noise (AWGN) channel, has the same performance as the system under consideration. A very promising mapping function, called the cumulant-generating function-based ESM ( $\kappa$ ESM), was introduced in [14]. This mapping function combines the simplicity of exponential ESM (EESM) with the accuracy of mutual information ESM (MIESM) [15]. Another advantage is that this mapping function can be used to optimize the coding rate together with the energy and bit allocation per subcarrier.

In [16], EESM has been applied to ACM in a multi-carrier system with feedback delays. The bit allocation per subcarrier and the code rate are selected such that the throughput gets maximized under a certain block error rate constraint. However, because the transmitter is unaware of the fact that the available CSI is delayed, the transmitter sometimes over- or underestimates the actual channel conditions which results in a loss of spectral efficiency. In [17], the throughput of a BIC-OFDM system is optimized under a target packet error rate (PER) constraint, where a packet can consist of multiple OFDM symbols. Also here, the considered adaptation algorithm at the transmitter does not account for CSI imperfections, which leads to a violation of the PER constraint when only delayed CSI is available.

*Rationale and contributions.* This paper deals with an ACM scheme for the SU link of a cognitive system based on a BIC-OFDM signaling with imperfect CSI at the SU transmitter, due to estimation errors or feedback delays. The performance metric we consider is the goodput (GP), which is similar to the throughput but considers only the number of information bits which are correctly received. The key idea behind the proposed method relies on

optimizing the long-term average GP of the SU link, averaged over the realizations of both the actual channel and the available CSI at the SU transmitter, under the constraints of the total transmitted energy and the level of interference on the PU receivers. This can be achieved by optimizing the expected GP (EGP) metric.<sup>1</sup> This optimal metric is the expected GP conditioned on the available CSI at the SU transmitter. In view of these features, our proposed scheme turns out to be more competitive, when compared to the current literature, as outlined in the sequel.

1. Instead of resorting to the often used information-theoretical capacity metric, a more practically relevant metric, i.e., the GP, is optimized, which gives the advantage of allowing the optimization of realistic modulation and coding formats.
2. Unlike the ad hoc approaches used in our previous work [19, 20], we now start from the optimal expression for the EGP. By using the statistical approximation for the effective SNR, which we introduced in [21], we now derive an analytical, tractable approximation for the EGP, which we call the approximate EGP (AEGP). In the numerical results, we show that the AEGP is a far more accurate approximation of the EGP, compared to the metrics used in [19, 20]. To the authors' knowledge, these works are the first ones which propose to use a practical metric, which takes care of the imperfect CSI, for the optimization of the transmission parameters.
3. In this work, we successfully combine the practical assumption of imperfect CSI with the accurate model of the effective SNR, which results in the AEGP metric. This AEGP metric, which takes care of the imperfect CSI, is proposed as the objective function of an OP to search for the optimal combination of the ACM parameters under the above mentioned transmit energy and interference constraints. By using the AEGP, packet errors or a loss in spectral efficiency by over- or underestimating the actual channel conditions are largely avoided. This differs from the approach taken in [16, 17], where the transmitter is unaware that its CSI is imperfect and only the impact of the imperfect CSI on the performance is investigated.
4. We derive several ACM solutions which optimize the code rate together with uniform or non-uniform bit allocation and uniform or non-uniform energy allocation. The performance of these algorithms is investigated for different types of CSI at the SU transmitter.
5. Although affected by imperfect CSI, extensive simulation runs show that the proposed ACM

algorithms allow significant gains compared to non-adaptive ACM schemes. Further, depending on the quality level of the CSI, the resulting GP performance can be very close to that obtainable in scenarios where perfect CSI is employed.

**Organization.** In Section 2, we describe the cognitive BIC-OFDM system. In Section 3, we introduce the EGP metric and discuss the statistical approximation of the  $\kappa$ ESM. The ACM algorithms which select the code rate and the energy and bit allocations per subcarrier are derived in Section 4. The accuracy of the EGP metric and the performance of the ACM algorithms are validated in Section 5. The conclusions are presented in Section 6.

**Notations.** Expectation operator is  $E[\cdot]$ ,  $[\cdot]^T$  is the transpose operator,  $[\cdot]^H$  is the Hermitian transpose operator,  $\mathbf{x} \sim \mathcal{CN}(0, \mathbf{\Sigma})$  refers to a circular symmetric zero-mean Gaussian complex random vector with covariance matrix  $\mathbf{\Sigma}$ , and the matrix  $\mathbf{I}$  denotes the identity matrix. The  $i$ th column of the identity matrix is denoted by  $\mathbf{e}_i$ . The notation  $(\mathbf{X})_{ij}$  refers to the element on the  $i$ th row and  $j$ th column of the matrix  $\mathbf{X}$ , while  $(\mathbf{x})_i$  denotes the  $i$ th component of the vector  $\mathbf{x}$ .

## 2 Cognitive BIC-OFDM system model

We consider a SU network, which consists of a point-to-point OFDM link, that occupies the same bandwidth as a PU network containing  $N_{\text{PU}}$  PU receivers. Messages are transmitted by means of a packet-oriented BIC-OFDM communication system consisting of  $N$  subcarriers within a bandwidth  $B$  [14]. Each packet contains  $N_p$  information bits and  $N_{\text{CRC}}$  bits for the cyclic redundancy check (CRC), which leads to a total of  $N_u = N_p + N_{\text{CRC}}$  bits per packet. These  $N_u$  bits are first encoded by a convolutional encoder. Several convolutional codes are available at the transmitter; these are punctured versions of a rate 1/2 code, designated by their rate  $r \in \mathcal{D}_r$ . In the following step, these  $N_u/r$  coded bits are randomly interleaved and Gray-mapped to  $N_s$  unit-energy quadrature amplitude modulation (QAM) symbols. In the last step, we make use of OFDM, with  $N$  available subcarriers per OFDM symbol, to transmit the  $N_s$  QAM symbols over a frequency-selective fading channel, which is assumed to be time-invariant for the whole packet transmission duration. The duration of an OFDM symbol will be denoted by  $T_s$ . The SU receiver first performs a fast Fourier transform (FFT) on the received OFDM symbol; the  $k$ th OFDM subcarrier, with  $k \in \{1, \dots, N\}$  is observed at the corresponding FFT output as

$$z_k \triangleq \sqrt{E_k} H_k x_k + w_k, \quad (1)$$

where  $E_k$  is the transmit energy on the  $k$ th subcarrier,  $H_k$  is the corresponding channel coefficient,  $x_k$  is the constellation symbol transmitted on subcarrier  $k$  containing  $m_k \in$

$\mathcal{D}_m$  coded bits and  $E[|x_k|^2] = 1$ , and  $w_k \in \mathcal{CN}(0, \sigma_w^2)$  is the additive noise contribution. The transmit energies are constrained by

$$\sum_{k=1}^N E_k \leq E_{\max} \quad (2)$$

where  $E_{\max}$  is the maximal transmit energy per OFDM symbol. Next, the SU receiver first performs soft demapping, and finally de-interleaves and decodes the packet; the CRC allows to verify whether the packet has been correctly decoded.

The received SNR associated with the  $k$ th subcarrier at the FFT output is defined as

$$\gamma_k \triangleq \frac{E_k |H_k|^2}{\sigma_w^2}. \quad (3)$$

Let us arrange the received SNRs into a vector  $\mathbf{\Gamma} \triangleq [\gamma_1, \dots, \gamma_N]$  for further use. We define the transmission mode (TM)  $\phi \triangleq \{\mathbf{m}, r\} \in \mathcal{D}_m^N \times \mathcal{D}_r$ , with  $\mathbf{m} \triangleq [m_1, \dots, m_N]^T$ . As not all  $N$  available subcarriers will necessarily be used for the transmission, we make a distinction between the set  $\{1, \dots, N\}$  of available subcarriers, and the set  $\mathcal{N} \subseteq \{1, \dots, N\}$  of active subcarriers. When the  $k$ th subcarrier is not active (i.e.,  $k \notin \mathcal{N}$ ), we have  $E_k = 0$  and  $m_k = 0$ .

Because of noise and/or feedback delays, the CSI available at the transmitter will often be imperfect. To make the description of our proposed approach quite general, we will denote the CSI, which is available at the transmitter about the actual channel realization  $\mathbf{H} \triangleq [H_1, \dots, H_N]^T$ , by the vector  $\mathbf{CSI}$ . We make the assumption that  $\mathbf{H}$  and  $\mathbf{CSI}$  are jointly zero-mean circular symmetric Gaussian. It then follows that  $\mathbf{H}$  conditioned on  $\mathbf{CSI}$  is Gaussian, with expectation  $\mu_{\mathbf{H}|\mathbf{CSI}} = E_{\mathbf{H}}[\mathbf{H}|\mathbf{CSI}]$  and covariance matrix  $\mathbf{C}_{\mathbf{H}|\mathbf{CSI}} = E_{\mathbf{H}}[\mathbf{H}\mathbf{H}^H|\mathbf{CSI}] - \mu_{\mathbf{H}|\mathbf{CSI}}\mu_{\mathbf{H}|\mathbf{CSI}}^H$ ; note that  $\mu_{\mathbf{H}|\mathbf{CSI}}$  is the minimum mean-squared error (MMSE) estimate of  $\mathbf{H}$  based on  $\mathbf{CSI}$ . Some examples of  $\mathbf{CSI}$  and the associated statistics are given in the Appendix section.

The signals transmitted in the SU network cause interference at the PU receivers, which should be constrained in order not to affect the PU QoS. Denoting by  $G_k^{(q)}$  the channel gain from the SU transmitter to the  $q$ th PU receiver, experienced by the  $k$ th subcarrier, the interference constraints can be expressed as  $\sum_{k \in \mathcal{N}} E_k |G_k^{(q)}|^2 \leq \mathcal{I}_q$  for  $q \in \mathcal{Q} \triangleq \{1, \dots, N_{\text{PU}}\}$ .

We denote by  $\mathbf{CSI}_{\text{PU}} = \{\mathbf{CSI}_{\text{PU}}^{(q)}, q \in \mathcal{Q}\}$  the imperfect CSI available at the SU transmitter about its channels to the PU receivers. This CSI could be obtained from a band manager [22] or, assuming time-division duplexing in the PU network and channel reciprocity, this CSI could be extracted by the SU transmitter when the considered

PU receiver has switched to a transmission mode. As only  $\mathbf{CSI}_{\text{PU}}$  and not the exact channel gains  $G_k^{(q)}$  are available at the SU transmitter, it can happen that the interference constraint at the PU receivers is violated. Therefore, alternative formulations of the interference constraints are needed that can be satisfied by the SU transmitter. A first possibility is to satisfy the interference constraints only on average, conditioned on the available  $\mathbf{CSI}_{\text{PU}}^{(q)}$ . In this case, the interference constraint is replaced by

$$E_{\mathbf{G}^{(q)}} \left[ \sum_{k \in \mathcal{N}} E_k |G_k^{(q)}|^2 \mid \mathbf{CSI}_{\text{PU}}^{(q)} \right] \leq \mathcal{I}_q, \quad \forall q \in \mathcal{Q}, \quad (4)$$

where  $\mathbf{G}^{(q)} \triangleq [G_1^{(q)}, \dots, G_N^{(q)}]^T$ . The expected value in (4) can be expressed as ( $\forall q \in \mathcal{Q}$ )

$$\begin{aligned} E_{\mathbf{G}^{(q)}} \left[ \sum_{k \in \mathcal{N}} E_k |G_k^{(q)}|^2 \mid \mathbf{CSI}_{\text{PU}}^{(q)} \right] \\ = \sum_{k \in \mathcal{N}} E_k \left( \left| \left( \boldsymbol{\mu}_{\mathbf{G} \mid \mathbf{CSI}_{\text{PU}}}^{(q)} \right)_k \right|^2 + \left( \mathbf{C}_{\mathbf{G} \mid \mathbf{CSI}_{\text{PU}}}^{(q)} \right)_{k,k} \right), \end{aligned} \quad (5)$$

where we have assumed that the distribution of  $\mathbf{G}^{(q)}$  conditioned on  $\mathbf{CSI}_{\text{PU}}^{(q)}$  is Gaussian with mean  $\boldsymbol{\mu}_{\mathbf{G} \mid \mathbf{CSI}_{\text{PU}}}^{(q)}$  and covariance matrix  $\mathbf{C}_{\mathbf{G} \mid \mathbf{CSI}_{\text{PU}}}^{(q)}$ .

A second possibility is to define the interference constraint by means of uncertainty sets [23, 24]. By defining the uncertainty set  $\mathcal{S}_k^{(q)}$  as follows

$$\mathcal{S}_k^{(q)} = \left\{ \hat{G}_k^{(q)} : \hat{G}_k^{(q)} = \left( \boldsymbol{\mu}_{\mathbf{G} \mid \mathbf{CSI}_{\text{PU}}}^{(q)} \right)_k + \alpha \epsilon, \|\epsilon\| \leq 1 \right\}, \quad (6)$$

the interference constraint is formulated as

$$\sum_{k \in \mathcal{N}} E_k |\hat{G}_k^{(q)}|^2 \leq \mathcal{I}_q, \quad \forall q \in \mathcal{Q}, \forall \hat{G}_k^{(q)} \in \mathcal{S}_k^{(q)} \quad (7)$$

where the complex scalar  $\alpha$  defines the size of the uncertainty interval, which directly influences the minimum probability that the interference is below the interference threshold  $\mathcal{I}_q$ . The set of constraints in (7) can be reduced to a single constraint per PU receiver, by only considering the value of  $\hat{G}_k^{(q)}$  in  $\mathcal{S}_k^{(q)}$  which leads to the most restrictive constraint. Denoting this value by  $G_k^{*(q)}$ , (7) is equivalent to

$$\sum_{k \in \mathcal{N}} E_k |G_k^{*(q)}|^2 \leq \mathcal{I}_q, \quad \forall q \in \mathcal{Q}. \quad (8)$$

A third possibility, used in [12, 25, 26], is to neglect the statistical variation of  $G_k^{(q)}$  for given  $\mathbf{CSI}_{\text{PU}}^{(q)}$ , and to use the following interference constraint

$$\sum_{k \in \mathcal{N}} E_k \left| \left( \boldsymbol{\mu}_{\mathbf{G} \mid \mathbf{CSI}_{\text{PU}}}^{(q)} \right)_k \right|^2 \leq \mathcal{I}_q, \quad \forall q \in \mathcal{Q}. \quad (9)$$

We note that these interference constraints can be linked to the concept of interference probability as defined in [12]. The interference probability (IP) for the  $q$ th PU receiver reads as

$$\text{IP}_q = \Pr \left( \sum_{k \in \mathcal{N}} E_k |G_k^{(q)}|^2 > \mathcal{I}_q \right). \quad (10)$$

In the case that the dynamically allocated energy vector  $\mathbf{E} \triangleq [E_1, \dots, E_N]^T$  leads to an intolerable IP, one can substitute  $\mathcal{I}_q$  in the corresponding interference constraint by  $\kappa_q \mathcal{I}_q$ . The scaling factor  $\kappa_q$  is chosen such that  $\text{IP}_q$  reaches an acceptable value, after finding a new dynamic allocation of the vector  $\mathbf{E}$  which satisfies the new constraint.

Finally, it is clear that the constraints (5), (8), and (9) all have the same mathematical form. This means that our proposed algorithms are compatible with all these constraints. For the remainder of the paper however, we will consider the average interference constraint (5).

### 3 Goodput performance metric

The goodput (GP), being defined as the ratio of the number of correctly received information bits (associated with correctly decoded packets) and the actual transmission time, has a very clear practical interpretation. Normalizing the GP by dividing by the actual bandwidth  $N/T_s$ , the GP corresponding to a given TM  $\phi = \{\mathbf{m}, r\}$  and SNR vector  $\boldsymbol{\Gamma}$  is expressed as

$$\text{GP} = \frac{N_p r}{NN_u} \left( \sum_{k \in \mathcal{N}} m_k \right) \cdot (1 - \text{PER}(\phi, \boldsymbol{\Gamma})), \quad (11)$$

where  $\text{PER}(\phi, \boldsymbol{\Gamma})$  is the packet error rate (PER) corresponding to the selected  $(\phi, \boldsymbol{\Gamma})$ . Note that the goodput (11) is a function of the actual channel realization  $\mathbf{H}$  because of (3). As a performance measure of the SU network, we consider the long-term average of the goodput (11) over many channel realizations.

If perfect CSI were available at the transmitter (i.e., the transmitter knows the realizations of its channels to the SU receiver and PU receivers), the optimal way of selecting the transmission mode  $\phi$  and the energy allocation vector  $\mathbf{E}$  as a function of these realizations is to maximize (11) under the constraints on the SU transmit energy and the interference at the PU receivers, for the given realizations  $\mathbf{H}$  and  $\{\mathbf{G}^{(q)}, q \in \mathcal{Q}\}$ . This selection obviously maximizes the long-term average goodput of the system, given by  $\text{GP}_{\text{avg}} = E_{\mathbf{H}, \{\mathbf{G}^{(q)}, q \in \mathcal{Q}\}} [\text{GP}]$ .

However, when only imperfect CSI is available, the transmission parameters  $(\phi, \mathbf{E})$  must be selected as functions of  $\mathbf{CSI}$  and  $\mathbf{CSI}_{\text{PU}}$ , rather than  $\mathbf{H}$  and  $\{\mathbf{G}^{(q)}, q \in \mathcal{Q}\}$ . Taking into account that for given  $\phi$  and  $\mathbf{E}$ , GP from (11) is a function of  $\mathbf{H}$  and that the joint probability density function of  $\mathbf{H}$ ,  $\mathbf{CSI}$ , and  $\mathbf{CSI}_{\text{PU}}$  can be factored as

$p(\mathbf{H}, \mathbf{CSI}, \mathbf{CSI}_{\text{PU}}) = p(\mathbf{H}|\mathbf{CSI})p(\mathbf{CSI})p(\mathbf{CSI}_{\text{PU}})$ , the long-term average goodput can be written as

$$\begin{aligned} \text{GP}_{\text{avg}} &= E_{\mathbf{H}, \mathbf{CSI}, \mathbf{CSI}_{\text{PU}}} [\text{GP}] \\ &= E_{\mathbf{CSI}, \mathbf{CSI}_{\text{PU}}} \left[ \frac{N_p r}{N N_u} \left( \sum_{k \in \mathcal{N}} m_k \right) \cdot (1 - E_{\mathbf{H}}[\text{PER}(\phi, \Gamma)|\mathbf{CSI}]) \right]. \end{aligned} \quad (12)$$

It follows from (12) that  $\text{GP}_{\text{avg}}$  becomes maximum when for given  $(\mathbf{CSI}, \mathbf{CSI}_{\text{PU}})$  the transmission parameters  $(\phi, E)$  maximize the expression between brackets in the second line of (12), under the constraints (2) and (4). This is equivalent to maximizing the expected goodput (EGP) metric, given by

$$\begin{aligned} \text{EGP} &= E_{\mathbf{H}} [\text{GP}|\mathbf{CSI}] \\ &= \frac{N_p r}{N N_u} \left( \sum_{k \in \mathcal{N}} m_k \right) \cdot (1 - E_{\mathbf{H}} [\text{PER}(\phi, \Gamma)|\mathbf{CSI}]). \end{aligned} \quad (13)$$

which is the conditional expectation of GP for given  $\mathbf{CSI}$  and represents the optimal performance metric in terms of  $\text{GP}_{\text{avg}}$  when only imperfect CSI is available at the transmitter.

The evaluation of  $\text{PER}(\phi, \Gamma)$  is not an easy task. In [14], an accurate link performance evaluation model, referred to as  $\kappa$ ESM, has been proposed for the BIC-OFDM system. This model provides a closed-form expression for the effective SNR  $\gamma$ . The effective SNR  $\gamma$  has the important property that the PER of the considered BIC-OFDM system where the SNRs and transmission mode of the subcarriers are given by  $\Gamma$  and  $\phi$ , respectively, is approximately equal to  $\text{PER}_{\text{ESM}}(r, \gamma)$ , which denotes the PER of an equivalent BPSK system (i.e., using the same convolutional code with rate  $r$ ) which operates over an AWGN channel with SNR equal to  $\gamma$ . The effective SNR is calculated as [14]

$$\gamma \triangleq -\beta \log(Y), \quad (14)$$

where  $\beta$  is a scaling coefficient which is optimized across all possible TMs [27].  $Y$  is expressed as

$$Y \triangleq \frac{1}{\sum_{l \in \mathcal{N}} m_l} \sum_{k \in \mathcal{N}} \Omega_k, \quad (15)$$

and  $\Omega_k$  is given by

$$\Omega_k \triangleq \sum_{n=1}^{\frac{\sqrt{2} m_k}{2}} \alpha_{k,n} e^{-\frac{\gamma_k n^2 d_{k,\min}^2}{4\beta}}, \quad (16)$$

where  $d_{k,\min}$  denotes the minimum Euclidean distance of the constellation used on the  $k$ th subcarrier, and  $\alpha_{k,n}$  is a known constant which depends on the chosen constellation.

The EGP from (13) can now be approximated by replacing  $\text{PER}(\phi, \Gamma)$  by  $\text{PER}_{\text{ESM}}(r, \gamma)$ , with  $\gamma$  given by

(14). The reference curves  $\text{PER}_{\text{ESM}}(r, \gamma)$  can be stored in a lookup table for each code rate  $r$  from the set  $\mathcal{D}_r$ . In order to compute the conditional expectation  $E_{\mathbf{H}} [\text{PER}_{\text{ESM}}(r, -\beta \log(Y))|\mathbf{CSI}]$ , we need the distribution of  $Y$  conditioned on  $\mathbf{CSI}$ . In [21], it was proposed to approximate  $Y$  conditioned on  $\mathbf{CSI}$  by a random variable  $Z$  which follows a beta distribution with shaping parameters  $a$  and  $b$ , i.e.,  $p_Z(z) \propto z^{a-1}(1-z)^{b-1}$  for  $0 \leq z \leq 1$ . The value of these shaping parameters is given by  $a = \frac{e(e-e^2-\nu)}{\nu}$  and  $b = \frac{(1-e)(e-e^2-\nu)}{\nu}$ , where  $e = E_{\mathbf{H}}[Y|\mathbf{CSI}]$  and  $\nu = \text{Var}_{\mathbf{H}}[Y|\mathbf{CSI}]$ . For more details, we refer to [21], where closed-form expressions were derived for  $e$  and  $\nu$ . Note that the distribution of  $Z$  depends on the selected bit allocation through the variables  $\alpha_{k,n}$ ,  $m_k$  and  $d_{k,\min}$ . Using this approximating beta distribution, we obtain the approximate EGP (AEGP) given by

$$\text{AEGP} = \frac{N_p r}{N N_u} \left( \sum_{k \in \mathcal{N}} m_k \right) \cdot (1 - E_Z [\text{PER}_{\text{ESM}}(r, -\beta \log(Z))]). \quad (17)$$

The expectation w.r.t.  $Z$  in (17) can be approximated by means of numerical integration.

## 4 Goodput optimization

In this section, we consider different algorithms the transmitter can employ to optimize the code rate  $r$ , the energy allocation  $E_k$  and the bit allocation  $m_k$  ( $\forall k \in \mathcal{N}$ ) such that the AEGP from (17) is maximized, while satisfying the transmit energy constraint (2) and the interference constraints (4) at the PU receivers. These algorithms assume that only imperfect CSI is available at the transmitter.

### 4.1 Uniform energy and bit allocation

In this first subsection, we make the restriction that the bit and energy allocation is uniform and that all  $N$  available subcarriers are actually used, i.e.,  $\mathcal{N} = \{1, \dots, N\}$ . For the bit and energy allocation, this means that

$$m_k = m, E_k = E, \quad \forall k \in \mathcal{N}, \quad (18)$$

where  $m \in \mathcal{D}_m$ . Considering the constraints (2) and (4), the optimal uniform energy per subcarrier is given by

$$E = \min \left( \min_{q \in \mathcal{Q}} \frac{\mathcal{I}_q}{E_{G^{(q)}} \left[ \sum_{k \in \mathcal{N}} |G_k^{(q)}|^2 |\mathbf{CSI}_{\text{PU}}^{(q)}| \right]}, \frac{E_{\max}}{|\mathcal{N}|} \right), \quad (19)$$

where the expected value can be found from (5) and  $|\mathcal{N}|$  denotes the number of active subcarriers. The transmitter will calculate the AEGP (17) for every TM  $\phi = \{m, r\}$ , and then selects the TM  $\phi = \{m, r\}$  which yields the largest AEGP. The pseudo-code of this optimization is outlined in Table 1.

**Table 1** Uniform energy and bit allocation

Optimization of $\mathbf{E}$ , $\mathbf{m}$ and $r$
<b>Set</b> $\text{AEGP}_{\text{opt}} = 0$
<b>Set</b> $\bar{E} = \min \left( \min_{q \in \mathcal{Q}} \frac{I_q}{\sum_{l \in \mathcal{N}} ( (\mathbf{h}_{\mathbf{g}(\text{csi})}^{(q)}) ^2 + (\mathbf{c}_{\mathbf{g}(\text{csi})}^{(q)}) )}, \frac{E_{\text{max}}}{ \mathcal{N} } \right)$
<b>For</b> $m \in \mathcal{D}_m$
<b>Set</b> $m_k = m, \quad \forall k \in \mathcal{N}$
<b>For</b> $r \in \mathcal{D}_r$
<b>Set</b> AEGP according to (17)
<b>If</b> $\text{AEGP} \geq \text{AEGP}_{\text{opt}}$ <b>Then</b>
<b>Set</b> $\text{AEGP}_{\text{opt}} = \text{AEGP}$
<b>Set</b> $r_{\text{opt}} = r$
<b>Set</b> $m_{\text{opt}} = m$
<b>End If</b>
<b>End For</b>
<b>End For</b>

#### 4.2 Optimized energy and uniform bit allocation

In this subsection, we will adapt the previous algorithm such that the transmitter optimizes the energy per subcarrier, while the bit allocation remains uniform. As explained further, we will allow some of the subcarriers to be inactive, i.e.,  $\mathcal{N} \subseteq \{1, 2, \dots, N\}$ . We first have a closer look at the EGP from (13) where  $\text{PER}(\phi, \Gamma)$  is replaced by  $\text{PER}_{\text{ESM}}(r, \gamma)$ , i.e.,

$$\text{EGP} \approx \frac{N_p r}{NN_u} \left( \sum_{k \in \mathcal{N}} m_k \right) \cdot (1 - E_{\mathbf{H}}[\text{PER}_{\text{ESM}}(r, -\beta \log(Y(\mathbf{E}))) | \mathbf{CSI}]), \quad (20)$$

where we have explicitly shown the dependence on the energy allocation vector  $\mathbf{E}$ . Because the PER is a convoluted function of the individual subcarrier energies, an exact optimization of this metric will be very hard to obtain. Therefore, we suggest a more computationally efficient method, by optimizing the following simplification of the EGP

$$\text{EGP} \approx \frac{N_p r}{NN_u} \left( \sum_{k \in \mathcal{N}} m_k \right) \cdot (1 - \text{PER}_{\text{ESM}}(r, -\beta \log(E_{\mathbf{H}}[Y(\mathbf{E}) | \mathbf{CSI}]))), \quad (21)$$

where the average is now taken inside the logarithm. As  $\text{PER}_{\text{ESM}}(r, \gamma)$  decreases with increasing  $\gamma$ , the maximization of (21) w.r.t.  $\mathbf{E}$  is equivalent to the minimization of  $E_{\mathbf{H}}[Y(\mathbf{E}) | \mathbf{CSI}]$ . The latter function can be obtained analytically [21]:

$$E_{\mathbf{H}}[Y(\mathbf{E}) | \mathbf{CSI}] = \frac{1}{\sum_{l \in \mathcal{N}} m_l} \sum_{k \in \mathcal{N}} \sum_{n=1}^{\frac{\sqrt{2} m_k}{2}} g_{k,n}(E_k), \quad (22)$$

where

$$g_{k,n}(E_k) = \alpha_{k,n} \frac{e^{-\frac{|\mu_{\mathbf{H}|\mathbf{CSI}}|_k|^2 \frac{E_k}{4\beta\sigma_w^2} n^2 d_{k,\min}^2}{1 + \frac{E_k}{4\beta\sigma_w^2} n^2 d_{k,\min}^2 (\mathbf{C}_{\mathbf{H}|\mathbf{CSI}})_{k,k}}}}{1 + \frac{E_k}{4\beta\sigma_w^2} n^2 d_{k,\min}^2 (\mathbf{C}_{\mathbf{H}|\mathbf{CSI}})_{k,k}}}. \quad (23)$$

So the optimized energy allocation that maximizes the simplified EGP in (21) is found by solving the following OP

$$\begin{cases} \mathbf{E}^{(\text{opt})} = \arg \min_{\mathbf{E}} \sum_{k \in \mathcal{N}} \sum_{n=1}^{\frac{\sqrt{2} m_k}{2}} g_{k,n}(E_k) \\ \text{s.t.} \quad \sum_{k \in \mathcal{N}} E_k \leq E_{\text{max}} \\ (4) \end{cases}. \quad (24)$$

According to [28], an OP is convex when both the constraints and the objective function are convex. From (24), it is clear that the constraints are convex, as they are linear in the components of  $\mathbf{E}$ . Further, the convexity of the objective function follows from the fact that the second derivative of  $g_{k,n}(E_k)$  with respect to  $E_k$  can be shown to be non-negative; hence, each term of the objective function is convex, so that the entire objective function is convex as well. Therefore, the OP of (24) can be efficiently solved by using optimization tools such as CVX [29].

For the optimization of the EGP, we slightly adapt the algorithm outlined in Table 1. We start by considering all available subcarriers as active, i.e.,  $\mathcal{N} = \{1, \dots, N\}$ . For every possible TM  $\phi = \{m, r\}$  the algorithm computes the approximation (17) of the EGP, using as energy allocation the solution of OP (24). Because the energy allocation now depends on the parameter  $m$ , it must now become part of the outer loop of the algorithm. For a given value of  $m$ , it might happen that for some  $k$  the optimized value of  $E_k$  equals 0. In this case, the corresponding subcarriers are removed from the active set  $\mathcal{N}$  by putting  $m_k = 0$ , which also removes the large terms with  $E_k = 0$  (i.e.,  $\gamma_k = 0$ ) from (15) for the considered bit allocation. Finally, the algorithm selects the TM and the corresponding energy allocation yielding the largest value of the AEGP (17).

#### 4.3 Uniform energy and greedy bit allocation

In this subsection we consider a uniform energy allocation according to (19) and an optimized bit allocation per subcarrier.

We first consider the simplified expression for the EGP (21):

$$\text{EGP} \approx \frac{N_p r}{NN_u} \left( \sum_{k \in \mathcal{N}} m_k \right) \cdot (1 - \text{PER}_{\text{ESM}}(r, -\beta \log(E_{\mathbf{H}}[Y(\mathbf{m}, \mathbf{E}) | \mathbf{CSI}]))), \quad (25)$$

where now the dependence on the bit and energy allocation vectors  $\mathbf{m}$  and  $\mathbf{E}$  is explicitly shown. Considering (15), we notice that the simplified EGP from

(25) only depends on the bit allocation through the quantity  $\sum_{k \in \mathcal{N}} E_{\mathbf{H}} [\Omega_k(m_k, E_k) | \mathbf{CSI}]$  and the sum  $\sum_{k \in \mathcal{N}} m_k \stackrel{\Delta}{=} M(\mathbf{m})$ . Because the PER is a decreasing function of the effective SNR  $\gamma$ , the maximal value of the simplified EGP, for a fixed value of  $M(\mathbf{m})$ , will be achieved for the bit allocation  $\mathbf{m}$  and energy allocation  $\mathbf{E}$  which minimizes

$$\begin{aligned} & \arg \min_{\mathbf{E}, \mathbf{m}} \sum_{k \in \mathcal{N}} E_{\mathbf{H}} [\Omega_k(m_k, E_k) | \mathbf{CSI}] \\ &= \arg \min_{\mathbf{E}, \mathbf{m}} \sum_{k \in \mathcal{N}} \sum_{n=1}^{\frac{\sqrt{2^{m_k}}}{2}} g_{k,n}(m_k, E_k). \end{aligned} \quad (26)$$

where  $g_{k,n}(m_k, E_k)$  is given by (23), and the dependence on  $m_k$  is shown explicitly. However, this represents a mixed integer programming problem, which is computationally very hard. In order to obtain a computationally efficient solution, we base our algorithm on the iterative suboptimal greedy algorithm described in [30].

In the current iteration, we modify the bit allocation from the previous iteration by adding 2 bits (because we restrict our attention to square QAM constellations, representing an even number of bits) to the subcarrier which leads to the smallest increase of  $\sum_{k \in \mathcal{N}} E_{\mathbf{H}} [\Omega_k(m_k, E_k) | \mathbf{CSI}]$ . For the resulting bit and energy allocation, we determine the code rate  $r$  which leads to the highest AEGP (17). The iterative algorithm is initialized with  $m_k = 0$  for all available subcarriers (yielding  $M(\mathbf{m}) = 0$ ) and continues until all  $N$  available subcarriers have  $m_{\max}$  bits (yielding  $M(\mathbf{m}) = m_{\max}N$ ), where  $m_{\max}$  is the largest allowed number of bits in the constellation. At that point, we select the code rate  $r$  and the energy and bit allocation which correspond to the value of  $M(\mathbf{m})$  for which the AEGP (17) is maximal.

Now, we outline how the increase of  $\sum_{k \in \mathcal{N}} E_{\mathbf{H}} [\Omega_k(m_k, E_k) | \mathbf{CSI}]$  is evaluated. Let us denote by  $\mathbf{m}$  the value of the bit allocation vector and by  $\mathcal{N}$  the set of active subcarriers, both referring to the previous iteration. We now introduce the quantity  $\delta_k^{(m_k+2)}(\mathbf{m})$  which is defined as the increase of (26) when the bit allocation on subcarrier  $k$  increases from  $m_k$  to  $m_k + 2$ . If subcarrier  $k$  was not active in the previous iteration (i.e.,  $m_k = 0$ ), the set of active subcarriers increases from  $\mathcal{N}$  (previous iteration) to  $\mathcal{N} \cup \{k\}$  (current iteration), yielding the increase

$$\begin{aligned} \delta_k^{(2)}(\mathbf{m}) &= E_{\mathbf{H}} \left[ \Omega_k(2, E_k(\mathbf{m} + 2\mathbf{e}_k)) \right. \\ & \left. + \sum_{l \in \mathcal{N}} (\Omega_l(m_l, E_l(\mathbf{m} + 2\mathbf{e}_k)) - \Omega_l(m_l, E_l(\mathbf{m}))) | \mathbf{CSI} \right], \end{aligned} \quad (27)$$

where  $\mathbf{E}(\mathbf{m})$  and  $\mathbf{E}(\mathbf{m} + 2\mathbf{e}_k)$  denote the uniform energy allocations from (19) corresponding to the bit allocations

$\mathbf{m}$  and  $\mathbf{m} + 2\mathbf{e}_k$ , respectively, related to the previous and the current iteration; because the corresponding set of active subcarriers has changed,  $\mathbf{E}(\mathbf{m})$  and  $\mathbf{E}(\mathbf{m} + 2\mathbf{e}_k)$  are different, which makes in (27) the summation over  $l$  nonzero. If subcarrier  $k$  was already active in the previous iteration (i.e.,  $m_k > 0$ ), we obtain

$$\begin{aligned} \delta_k^{m_k+2}(\mathbf{m}) &= E_{\mathbf{H}} [\Omega_k(m_k + 2, E_k(\mathbf{m} + 2\mathbf{e}_k)) \\ & - \Omega_k(m_k, E_k(\mathbf{m})) | \mathbf{CSI}]. \end{aligned} \quad (28)$$

As in this case, the set of active subcarriers equals  $\mathcal{N}$  for both the previous and the current iteration, the uniform energy allocation from (19) satisfies  $\mathbf{E}(\mathbf{m} + 2\mathbf{e}_k) = \mathbf{E}(\mathbf{m})$ . In the current iteration, the increments  $\delta_k^{m_k+2}(\mathbf{m})$  are computed for all  $k \in \{1, \dots, N\}$ ; then, the subcarrier  $k$  which yields the lowest  $\delta_k^{m_k+2}(\mathbf{m})$  ( $k \in \{1, \dots, N\}$ ) is selected, and the bit allocation for this subcarrier and  $M(\mathbf{m})$  are both increased by 2, compared to the previous iteration.

#### 4.4 Suboptimal joint energy and bit allocation

The greedy bit allocation algorithm introduced in the previous subsection requires the reevaluation of the values of  $\delta_k^{m_k+2}(\mathbf{m})$  ( $\forall k \in \{1, \dots, N\}$ ) each time the set  $\mathcal{N}$  of active subcarriers is modified. The complexity would increase even further if we combined each step of the greedy bit allocation algorithm with the optimized energy allocation introduced in Section 4.2, which requires solving a convex optimization algorithm instead of a simple evaluation of Eq. (19).

To circumvent this complexity, we present a faster, less computationally intensive algorithm. We initialize the algorithm with the optimal uniform energy and bit allocation from Section 4.1. Then, as a first step we calculate for this specific uniform bit allocation the optimized energy allocation vector resulting from OP (24), for  $\mathcal{N} = \{1, \dots, N\}$ . In the second step, we optimize the bit allocation and code rate according to the greedy algorithm outlined in 4.3. Because during this step the energy allocation vector  $\mathbf{E}$  is kept to its value resulting from the previous step, we can drop the dependency of  $\delta_k^{m_k+2}$  on  $\mathbf{m}$  because  $\delta_k^{m_k+2}$  now depends only on  $m_k$  for given  $k$  and, therefore, has to be evaluated only once for each  $m_k$  ( $m_k \geq 0, \forall k \in \{1, \dots, N\}$ ). This considerably reduces the complexity. For more details, we refer to the pseudocode of this algorithm shown in Table 2. As a final step, the optimized energy allocation vector  $\mathbf{E}$  is recalculated according to Section 4.2, for the optimized TM resulting from the second step. The resulting values for the code rate  $r$ , energy allocation  $\mathbf{E}$ , and bit allocation  $\mathbf{m}$  are then used for the transmission.

**Table 2** Suboptimal joint energy and bit allocation

Optimization of $\mathbf{E}$ , $\mathbf{m}$ and $r$
<b>Set</b> $\text{AEGP}_{\text{opt}} = 0$
<b>Set</b> $r$ and $\mathbf{m}$ according to section 4.1
<b>Set</b> $\mathbf{E}$ according to (24)
<b>For</b> $k \in \{1, \dots, N\}$
<b>For</b> $m_k \in \mathcal{D}_m$
<b>Set</b> $\delta_k^{m_k}$ according to (28)
<b>End For</b>
<b>Set</b> $\delta_k^{m_{\max}+2} = \infty$
<b>End For</b>
<b>Set</b> $m_k = 0 (\forall k \in \{1, \dots, N\})$
<b>For</b> $M \in \{2, 4, \dots, m_{\max}N\}$
<b>Set</b> $k = \arg \min\{\delta_1^{m_1+2}, \dots, \delta_N^{m_N+2}\}$
<b>Set</b> $m_k = m_k + 2$
<b>Update</b> $\mathcal{N}$
<b>For</b> $r \in \mathcal{D}_r$
<b>Set</b> AEGP according to (17)
<b>If</b> $\text{AEGP} \geq \text{AEGP}_{\text{opt}}$ <b>Then</b>
<b>Set</b> $\text{AEGP}_{\text{opt}} = \text{AEGP}$
<b>Set</b> $r_{\text{opt}} = r$
<b>Set</b> $\mathbf{m}_{\text{opt}} = \mathbf{m}$
<b>End If</b>
<b>End For</b>
<b>End For</b>
<b>Set</b> $\mathbf{E}$ according to (24)

## 5 Numerical results

We consider a communication system characterized by the parameters from Table 3, which uses orthogonal frequency-division multiple access (OFDMA) to support several users. Here, we concentrate on the performance of a user to which 48 data subcarriers are allocated, which is equal to one subchannel in the FUSC permutation mode of WiMax [31]. These subcarriers are considered to be evenly spaced across the available bandwidth. The channel impulse responses behave according to the ITU vehicular A model [32], with time variations according to Jakes' model [33]. We consider a single PU receiver (so we can drop the index  $q$ ) and the channels between the different nodes are characterized by  $\text{Tr}(\mathbf{E}[\mathbf{h}\mathbf{h}^H]) = 1$  and  $\text{Tr}(\mathbf{E}[\mathbf{g}\mathbf{g}^H]) = 10^{-3}$ , where  $\mathbf{h}$  and  $\mathbf{g}$  denote the channel impulse responses corresponding to the channel frequency responses  $\mathbf{H}$  and  $\mathbf{G}$ , respectively; this yields  $E[|H_k|^2] = 1$  and  $E[|G_k|^2] = 10^{-3}$  for  $k \in \{1, \dots, N\}$ . In this section, we will consider three types of CSI, i.e., estimated CSI, delayed CSI, and estimated and delayed CSI (see the Appendix section); we always assume that for both  $\mathbf{CSI}$  and  $\mathbf{CSI}_{\text{PU}}$ , the same type of CSI is avail-

**Table 3** System parameters

Data subcarriers ( $N$ )	48
Sampling rate ( $1/T$ )	5.6 MHz
FFT size ( $N_{\text{car}}$ )	512
Length of cyclic prefix ( $\nu$ )	64
Convolutional code	(133, 171) <sub>8</sub>
Code rates ( $\mathcal{D}_r$ )	1/2, 2/3, 3/4, 5/6
Constellation sizes ( $\mathcal{D}_m$ )	2, 4, 6 bits
Information bits ( $N_p$ )	1024
CRC ( $N_{\text{CRC}}$ )	32

able at the transmitter. We note however that this is not a requirement for the proper functioning of our proposed algorithms.

The SNR is defined as

$$\text{SNR} \triangleq \frac{E_{\text{max}}}{N\sigma_w^2}. \quad (29)$$

As a performance indicator for the different resource allocation schemes, we will display (12), which denotes the average of the actual GP w.r.t. the joint probability density function of  $\mathbf{H}$ ,  $\mathbf{CSI}$ , and  $\mathbf{CSI}_{\text{PU}}$ . This averaging involves the generation of realizations of  $\mathbf{CSI}$  and  $\mathbf{CSI}_{\text{PU}}$ , from which the corresponding  $(\mathbf{m}, \mathbf{E}, r)$  are computed. For each such realization of  $(\mathbf{m}, \mathbf{E}, r)$ , we generate realizations of  $\mathbf{H}$  according to the conditional distribution  $p(\mathbf{H}|\mathbf{CSI})$ . For each such realization of  $\mathbf{H}$ , we transmit and decode one packet using the transmission parameters  $(\mathbf{m}, \mathbf{E}, r)$  and verify whether a decoding error has occurred; averaging the indicator of a decoding error over the realizations of  $\mathbf{H}$  yields  $E_{\mathbf{H}}[\text{PER}(\phi, \Gamma)|\mathbf{CSI}]$  corresponding to the considered realization of  $(\mathbf{m}, \mathbf{E}, r)$ .

### 5.1 Accuracy of AEGP

In this subsection, we investigate how accurately the AEGP metric (17) approximates the EGP from (13). As a reference, we compare the accuracy with the predicted GP (PGP) introduced in [20] and the IC- $\kappa$ ESM introduced in [19]. The PGP is obtained by neglecting the uncertainty on  $\mathbf{H}$  given the actual CSI, and is calculated by substituting  $\mathbf{H}$  by  $\mu_{\mathbf{H}}|\mathbf{CSI}$  in the expression (15) and using this deterministic value of  $Y$  to replace the random variable  $Z$  in (17). The IC- $\kappa$ ESM is an approximation that only applies to delayed CSI. For this reason, we will compare the accuracy of these three metrics for the scenario where the transmitter only has delayed CSI available (see the "Delayed CSI" section in the Appendix). The following simulation parameters are used:  $\text{SNR} = 10$  dB,  $\mathcal{I}_q/\sigma_w^2 = 0$  dB, and the value of  $f_d\tau_d$  is equal to 0.05.

We generate 1000 realizations of  $\mathbf{CSI}$  and  $\mathbf{CSI}_{\text{PU}}$  (see the Appendix section), and for each realization, the corresponding optimum uniform bit and energy allocation and



code rate are obtained as described in Section 4.1. Then, for each realization of  $\mathbf{CSI}$ ,  $\mathbf{CSI}_{\text{PU}}$ , and the corresponding  $(m, E, r)$ , we compute (i) the AEGP from (17); (ii) the PGP; (iii) the IC- $\kappa$ ESM; (iv) the EGP from (13), where the average conditioned on  $\mathbf{CSI}$  is replaced by an arithmetical average over 1000 realizations of  $\mathbf{H}$ , generated according to the conditional distribution  $p(\mathbf{H}|\mathbf{CSI})$  (see the Appendix section), and for each realization of  $\mathbf{H}$ , it is verified whether the received packet is correctly decoded; and (v) the differences  $\epsilon_{\text{AEGP}} = |\text{AEGP} - \text{EGP}|$ ,  $\epsilon_{\text{PGP}} = |\text{PGP} - \text{EGP}|$ , and  $\epsilon_{\text{IC-}\kappa\text{ESM}} = |\text{IC-}\kappa\text{ESM} - \text{EGP}|$ . Table 4 shows the average, the standard deviation, and the root mean-squared (rms) value of  $\epsilon_{\text{AEGP}}$ ,  $\epsilon_{\text{PGP}}$ , and  $\epsilon_{\text{IC-}\kappa\text{ESM}}$ , resulting from the simulations; these numbers should be compared to the average of EGP over the CSI, which equals 1.42 bits/s/Hz. From Table 4, we observe that the AEGP is a very accurate estimate of the EGP, outperforming both the PGP and the IC- $\kappa$ ESM by about one order of magnitude in terms of rms value. This result validates the accuracy of both the  $\kappa$ ESM and our approximation of  $Y$  by a beta-distributed random variable. The high accuracy of the AEGP metric makes it a very attractive objective function for the optimization of the SU transmission parameters. Further, we also note that being able to accurately describe the expected performance of a link will also have further benefits for more high level algorithms such as scheduling as the probability, of correctly allocating a user to a channel that satisfies its demands, will be increased.

## 5.2 Uniform energy and bit allocation

The performance of the uniform energy and bit allocation algorithm described in Section 4.1 is investigated. As a reference, we will also show the performance in the case of perfect CSI and also for non-adaptive transmission.

In the case of perfect CSI, the optimal uniform energy allocation is given by

$$E = \min \left( \min_{q \in \mathcal{Q}} \frac{\mathcal{I}_q}{\sum_{l \in \mathcal{N}} |G_l^{(q)}|^2}, \frac{E_{\max}}{|\mathcal{N}|} \right). \quad (30)$$

Using this uniform energy allocation, the GP metric (11) is computed for each possible TM  $\{m, r\}$  but with  $\text{PER}(\phi, \mathbf{\Gamma})$  replaced by  $\text{PER}_{\text{ESM}}(r, \gamma)$ . The TM which corresponds to the largest GP is then considered optimal.

**Table 4** Accuracy of the AEGP, PGP and IC- $\kappa$ ESM metric (SNR= 10 dB,  $\mathcal{I}_q/\sigma_w^2 = 0$  dB and  $f_d\tau_d = 0.05$ )

	AEGP	PGP	IC- $\kappa$ ESM
$E[\epsilon]$	$1.87 \times 10^{-2}$	$5.48 \times 10^{-1}$	$5.57 \times 10^{-1}$
$\sqrt{\text{Var}[\epsilon]}$	$2.07 \times 10^{-2}$	$2.45 \times 10^{-1}$	$1.95 \times 10^{-1}$
$\sqrt{E[\epsilon^2]}$	$2.79 \times 10^{-2}$	$6.00 \times 10^{-1}$	$5.90 \times 10^{-1}$

In the case of non-adaptive transmission, the transmitter has no CSI available. This is equivalent to the case where the pdf of the channel gains conditioned on the CSI reduces to the unconditional pdf of the channel gains. Hence, the uniform energy allocation is obtained as

$$E = \min \left( \min_{q \in \mathcal{Q}} \frac{\mathcal{I}_q}{E_{G^{(q)}} \left[ \sum_{l \in \mathcal{N}} |G_l^{(q)}|^2 \right]}, \frac{E_{\max}}{|\mathcal{N}|} \right). \quad (31)$$

For the above energy allocation, the transmitter selects, for the current value of SNR (29), the TM  $\{m, r\}$  which leads to the highest value of  $E_{\mathbf{H}}[\text{GP}]$ , with GP given by (11).

Now, we will apply the algorithm described in Section 4.1. As a first example, we assume that the transmitter only has estimated CSI available (see the ‘‘Estimated CSI’’ section in the Appendix). The variance of the estimation error related to the PU and SU channels is equal to  $\sigma_e^2 = 0, 10, 20$ , and 30 dB. For the interference threshold, we consider  $\mathcal{I}_q/\sigma_w^2 = 0$  dB. The results are shown in Fig. 1. We observe that the performance of the SU network clearly depends on the variance of the estimation error  $\sigma_e^2$ . For  $\sigma_e^2 = 30$  dB, there is almost no gain by exploiting CSI compared to a non-adaptive transmission algorithm, because the CSI is unreliable. However, when the value of  $\sigma_e^2$  decreases, we consistently see a clear gain in performance by exploiting the CSI. When  $\sigma_e^2 = 0$  dB, we notice there is a negligible difference between the algorithm using estimated CSI or perfect CSI. Further, we also note that there is almost no gain compared to non-adaptive transmission for small SNR.

In the following example, the transmitter only has access to delayed CSI (see the ‘‘Delayed CSI’’ section in the Appendix). The performance of the SU network is shown

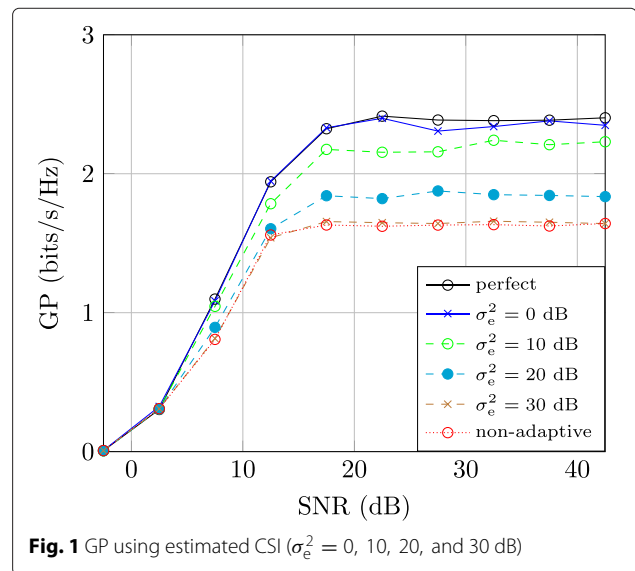


**Fig. 1** GP using estimated CSI ( $\sigma_e^2 = 0, 10, 20$ , and 30 dB)

in Fig. 2 for a value of  $f_d \tau_d$  equal to 0.01, 0.05, 0.1, and 0.2. It is clear from Fig. 2 that when  $f_d \tau_d$  is equal to 0.2, there is almost no gain in performance compared to the non-adaptive transmission algorithm because the channel variations are too fast. However, for lower values of  $f_d \tau_d$ , the GP of the SU network increases considerably. When  $f_d \tau_d = 0.01$ , the GP almost equals the performance of the algorithm which uses perfect CSI.

In Fig. 3, we show the difference in performance between optimizing the AEGP, the PGP (as in [20]), and the IC- $\kappa$ ESM (as in [19]). We show the performance for  $f_d \tau_d$  equal to 0.05 and 0.2. For  $f_d \tau_d = 0.05$ , we can see a small performance benefit by optimizing the AEGP compared to the less accurate PGP and IC- $\kappa$ ESM. When  $f_d \tau_d = 0.2$ , we notice that the performance improvement we get by using the AEGP or IC- $\kappa$ ESM becomes significantly larger compared to using the PGP. In this case, the performance achieved by using the PGP drops even below the performance we would get by using the non-adaptive approach. This demonstrates that the PGP approximation is unable to accurately describe the expected goodput and is thus not suited as an objective function for the OPs, especially in the case of fast channel variations. While optimizing the IC- $\kappa$ ESM is shown to achieve a similar performance as the optimization of the AEGP, the IC- $\kappa$ ESM is far less general than the proposed AEGP as it can only be used in the scenario with delayed CSI described in the “Delayed CSI” section in the Appendix.

In the last example, we combine the delayed CSI with the estimated CSI (see the “Estimated and delayed CSI” section in the Appendix). We choose  $f_d \tau_d = 0.2$  and  $\sigma_e^2 = 0$  dB. We investigate the performance for a different number ( $P$ ) of available, delayed channel estimates, with corresponding delays  $\tau_d, 2\tau_d, \dots, P\tau_d$ . The performances

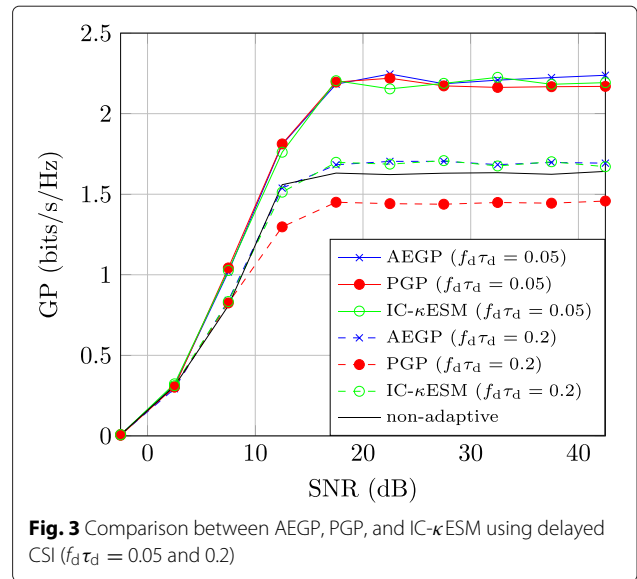


**Fig. 3** Comparison between AEGP, PGP, and IC- $\kappa$ ESM using delayed CSI ( $f_d \tau_d = 0.05$  and  $0.2$ )

are shown in Fig. 4 for  $P = 1, 2, 3$ , and 4. We observe that the performance of the SU network can be significantly improved when the CSI consists of multiple delayed channel estimates. In this example, the GP increases by about 20 % when going from  $P = 1$  to  $P = 4$  for high SNRs. We note that it is not possible to reach the performance of an algorithm with perfect CSI, by increasing the number of estimates. As is clear from Fig. 4, there is no noticeable performance gain by going from  $P = 3$  to  $P = 4$ .

In Fig. 5, we investigate the impact of the interference threshold. We show the performance of the uniform bit and energy allocation algorithm when  $\mathcal{I}_q/\sigma_w^2 = 0, 5$  and 10 dB. The resulting goodput is shown for the following simulation variables:  $f_d \tau_d = 0.2, \sigma_e^2 = 0$  dB

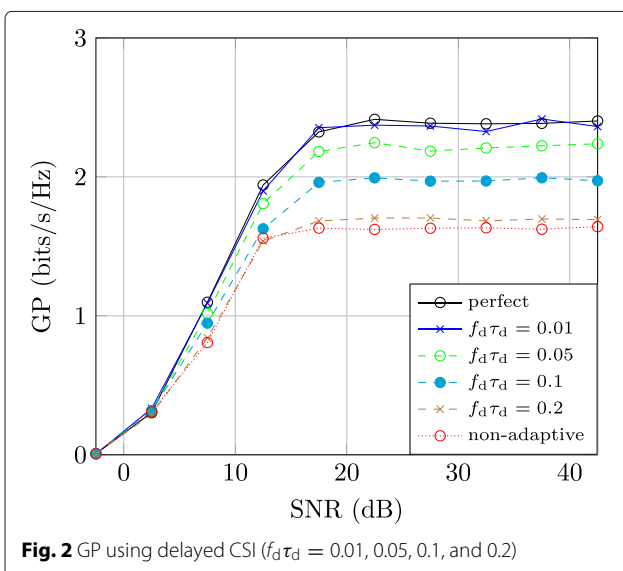


**Fig. 2** GP using delayed CSI ( $f_d \tau_d = 0.01, 0.05, 0.1$ , and  $0.2$ )

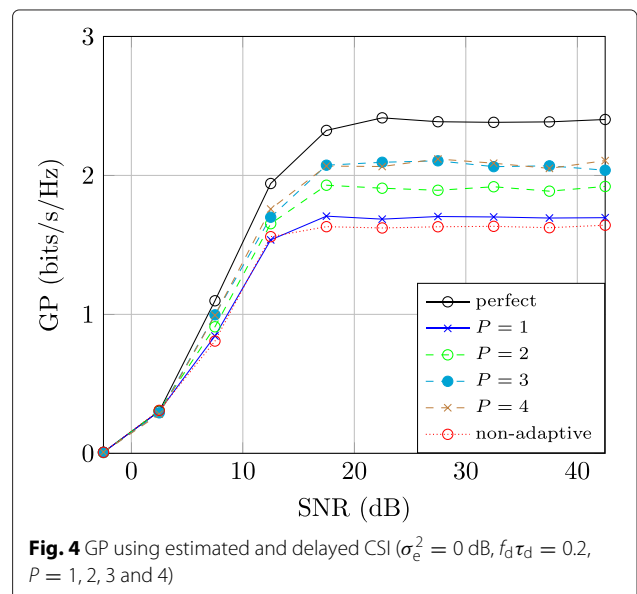
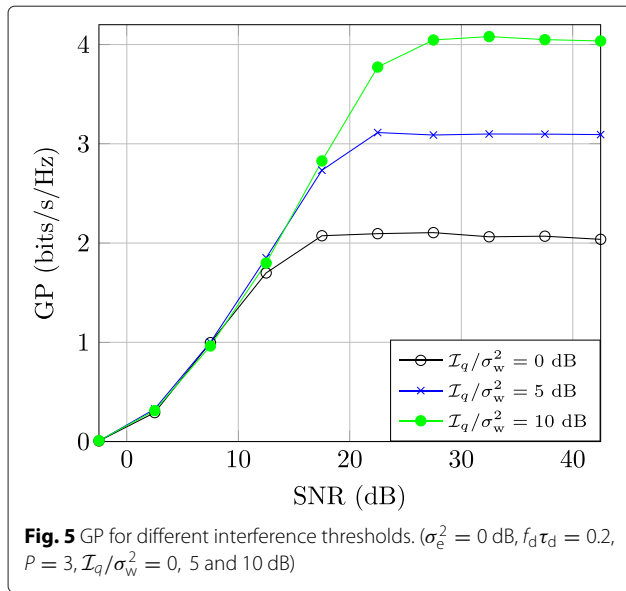


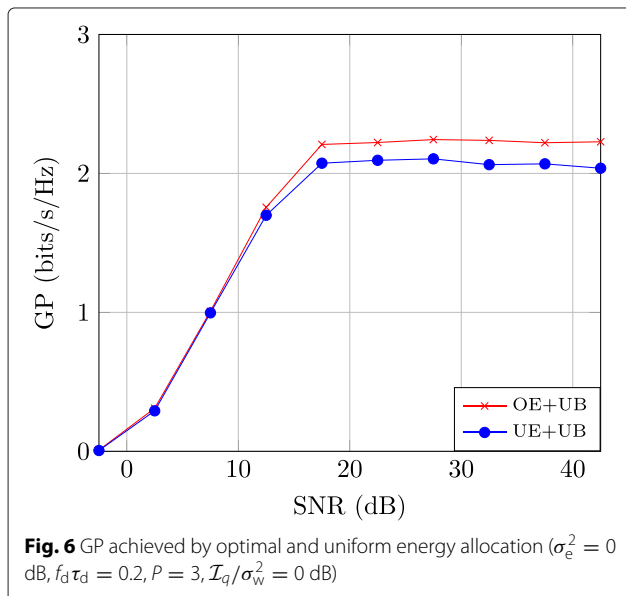
**Fig. 4** GP using estimated and delayed CSI ( $\sigma_e^2 = 0$  dB,  $f_d \tau_d = 0.2$ ,  $P = 1, 2, 3$  and  $4$ )



and  $P = 3$ . We observe that the value of the interference threshold has a huge impact on the performance of the SU network. A too conservative value of the interference threshold will severely limit the achievable goodput of the SU network.

**5.3 Optimized energy and uniform bit allocation**

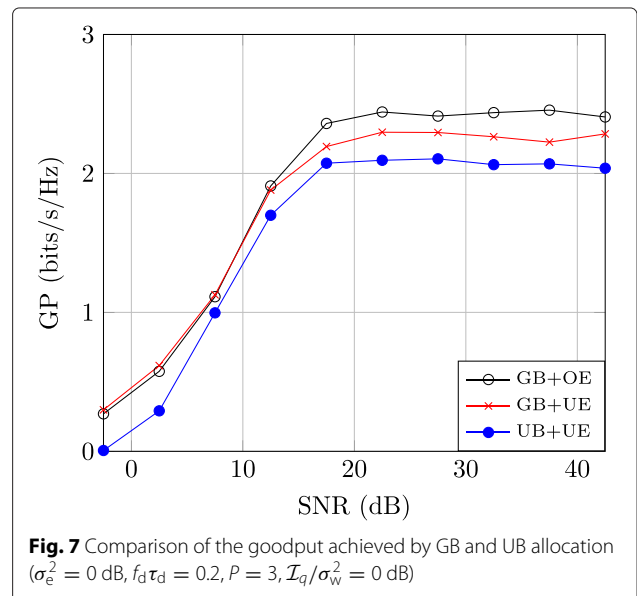
In this subsection, the optimized energy (OE) allocation from (24) and the uniform energy (UE) allocation are compared in terms of goodput. The following simulation parameters are chosen:  $\sigma_e^2 = 0$  dB,  $f_d \tau_d = 0.2$ ,  $P = 3$ , and  $I_q/\sigma_w^2 = 0$  dB. Figure 6 shows the goodput resulting from the uniform energy and bit allocation described



in Section 4.1, along with the goodput corresponding to the OE allocation for the same uniform bit (UB) allocation. We notice that for high SNR the OE allocation improves the goodput by about 8 % compared to UE allocation.

**5.4 Greedy bit allocation**

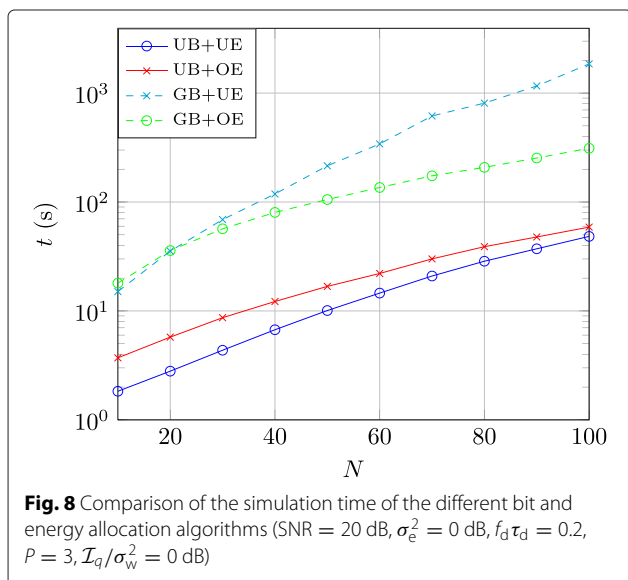
Now, we investigate the performance of the SU network in the case where the SU transmitter optimizes the bit allocation per subcarrier. The simulation parameters are chosen as follows:  $\sigma_e^2 = 0$  dB,  $f_d \tau_d = 0.2$ ,  $P = 3$ , and  $I_q/\sigma_w^2 = 0$  dB. We compare the performance of uniform bit and energy allocation (UB+UE), with our algorithm introduced in Section 4.3 which combines greedy bit allocation with uniform energy allocation (GB+UE). Further, we also consider the performance of the suboptimal algorithm introduced in Section 4.4 which combines the greedy bit allocation and optimized energy allocation (GB+OE). From Fig. 7, we notice that there is a considerable increase in GP when we apply GB instead of UB allocation. At low SNR, the transmitter is now capable of deactivating subcarriers with poor instantaneous channel gains, which considerably decreases the PER and improves GP. At higher SNR the transmitter can now better utilize the full capacity at each subcarrier by allocating a larger number of bits to a subcarrier with favorable channel gains. An even larger gain at higher SNR can be obtained by combining the GB with the OE allocation. In Fig. 7, we notice that the gain compared to uniform bit and energy allocation (UB+UE) amounts to 10 % for greedy bit and uniform energy allocation (GB+UE) and becomes nearly 20 % for greedy bit and optimized energy allocation (GB+OE). This additional gain is achieved by giving the



transmitter the freedom of reallocating the energy over the subcarriers, which improves the performance in several ways: it can happen for example that subcarriers with less favorable channel gains now receive more energy, or that subcarriers causing strong interference at the PU are switched off to allow for a higher total transmit energy. We do notice however that at lower SNRs the GB+OE algorithm performs slightly worse than the GB+UE algorithm. This is a consequence of our suboptimal approach outlined in Section 4.4. However, the performance loss at low SNR is very small, and an optimal joint bit and energy allocation algorithm would require a much higher complexity.

### 5.5 Computational complexity

To illustrate their complexity, we will compare the average computation times of the different resource allocation algorithms described in Section 4. The SNR is fixed at 20 dB and the simulation parameters are  $\sigma_e^2 = 0$  dB,  $f_d \tau_d = 0.2$ ,  $P = 3$  and  $\mathcal{I}_q/\sigma_w^2 = 0$  dB. In Fig. 8, the computation time of the algorithms is shown as a function of the number of subcarriers  $N$ . We notice a slight increase in computation time for the optimized energy allocation (UB+OE) compared to the uniform energy allocation (UB+UE). However, a more significant increase in computation time occurs when implementing the greedy bit allocation. The greedy bit with uniform energy allocation (GB+UE) described in Section 4.3 clearly becomes unfeasible when the number of subcarriers becomes too high. Compared to GB+UE, the complexity is significantly reduced when using the suboptimal joint energy and bit allocation (GB+OE) described in Section 4.4, whose computation time increases much more slowly with  $N$ .



## 6 Conclusions

In this paper, we have considered adaptive coding and modulation in a cognitive BIC-OFDM system, under the realistic assumption that only imperfect CSI is available. In order to tackle this problem, we introduced an optimum performance metric called the expected goodput (EGP), which is the expectation of the goodput, conditioned on the imperfect CSI.

A major advantage of this metric is that it allows the transmitter to account for the imperfections of the CSI by selecting its transmission parameters such that the best average goodput is achieved. To make the optimization of the code rate, bit and energy allocation tractable, we proposed a very accurate approximation of this performance metric, referred to as approximate EGP (AEGP). The numerical results clearly show that the ACM algorithms based on the AEGP have at least the same performance as the non-adaptive algorithms and, in most cases, clearly outperform them. Finally, we also show that, depending upon the quality of the available CSI, the proposed algorithms can come very close to the performance of algorithms with perfect CSI.

### Endnotes

<sup>1</sup>This EGP metric is different from the expected effective goodput metric proposed in [18]. The metric introduced in [18] takes into account the expected transmission time, which can vary because of the possibilities of retransmissions. It has however nothing to do with imperfect CSI which is the focus of the present paper.

<sup>2</sup>Note that if we have a number of paths  $L < \nu + 1$ , only  $L$  diagonal elements of  $\mathbf{R}_h$  are strictly greater than 0.

## Appendix

### Examples of different types of CSI at the transmitter

In the following, the impulse response of a generic channel between the SU transmitter and any receiver of the PU or SU network will be denoted by  $h(m, t)$ , where the delay variable is represented by the discrete time index  $m$  associated with a sampling rate  $1/T$ , and the time variability of the channel is indicated by a continuous time index  $t$ . Without any loss of generality, we can assume that  $h(m, t) = 0$  for  $m < 0$  and for  $m > \nu$ , where  $\nu$  is defined as the length of the cyclic prefix. For given  $t$ , the samples  $h(m, t)$  ( $0 \leq m \leq \nu$ ) of the channel impulse vector  $\mathbf{h}(t) \triangleq [h(0, t), \dots, h(\nu, t)]^T$  are assumed to be independent circular symmetric zero-mean Gaussian complex random variables; assuming stationarity w.r.t. the variable  $t$ , the covariance matrix of  $\mathbf{h}(t)$  is given by<sup>2</sup>  $\mathbf{R}_h \triangleq \text{diag}(\sigma_0^2, \dots, \sigma_\nu^2)$ . The time variations of the channel are described by Jakes' model [33], which gives  $E[h(m, t + \tau_d)h^*(m, t)] = J_0(2\pi f_d \tau_d) \sigma_m^2$ , where  $J_0(x)$

represents the zeroth-order Bessel function of the first kind, and  $f_d$  denotes the Doppler spread.

Introducing the Fourier matrix  $\mathbf{F} \in \mathbb{C}^{N_{\text{car}} \times (\nu+1)}$  as

$$\mathbf{F}_{k,l} \triangleq e^{-j2\pi(k-1)(l-1)/N_{\text{car}}}, \quad k = 1, \dots, N_{\text{car}}; l = 1, \dots, \nu+1, \quad (32)$$

the time-varying frequency response of the channel can then be written as  $\mathbf{H}(t) = \mathbf{F}\mathbf{h}(t)$  which has the covariance matrix  $\mathbf{R}_{\mathbf{H}} = \mathbf{F}\mathbf{R}_h\mathbf{F}^H$ . The  $k$ th component of  $\mathbf{H}(t)$  denotes the channel gain which affects the  $k$ th subcarrier at time instant  $t$ .

In the following subsections, we consider a few possible examples of the type of CSI available at the transmitter. Each case leads to different expressions for the parameters  $\mu_{\mathbf{H}|\text{CSI}}$  and  $\mathbf{C}_{\mathbf{H}|\text{CSI}}$ , which completely describe the random variable  $\mathbf{H}(t)$  conditioned on the available CSI as follows

$$\mathbf{H}(t) = \mu_{\mathbf{H}|\text{CSI}}(t) + \mathbf{n}(t), \quad (33)$$

where  $\mathbf{n}(t) \sim \mathcal{CN}(0, \mathbf{C}_{\mathbf{H}|\text{CSI}})$ . The probability density function  $p(\mathbf{H}(t)|\text{CSI})$  is then given by  $\mathcal{CN}(\mu_{\mathbf{H}|\text{CSI}}(t), \mathbf{C}_{\mathbf{H}|\text{CSI}})$ . If only  $N$  of the  $N_{\text{car}}$  subcarriers are available at the transmitter, as is the case in the numerical section, we can define a smaller  $\mu_{\mathbf{H}|\text{CSI}}$  and  $\mathbf{C}_{\mathbf{H}|\text{CSI}}$  which only contain the elements corresponding to the available subcarriers.

#### Estimated CSI

In this subsection we determine the quantities  $\mu_{\mathbf{H}|\text{CSI}}$  and  $\mathbf{C}_{\mathbf{H}|\text{CSI}}$  in the case of channel estimation errors. The transmitter only has access to an estimated frequency response  $\tilde{\mathbf{H}}(t)$ , which means that  $\text{CSI} = \tilde{\mathbf{H}}(t)$ . The estimated frequency response  $\tilde{\mathbf{H}}(t)$  is decomposed as

$$\tilde{\mathbf{H}}(t) = \mathbf{H}(t) + \tilde{\mathbf{e}}(t), \quad (34)$$

where  $\tilde{\mathbf{e}}(t)$  and  $\mathbf{H}(t)$  are statistically independent,  $\tilde{\mathbf{e}}(t) \sim \mathcal{CN}(0, \sigma_e^2 \mathbf{I}_{N_{\text{car}}})$ . In Section 5, we will use the value of the normalized estimation error variance  $\sigma_e^2 \triangleq \sigma^2 / \text{Tr}(\mathbf{E}[\mathbf{h}\mathbf{h}^H])$ . It can be shown that

$$\mu_{\mathbf{H}|\text{CSI}} = \mathbf{R}_{\mathbf{H}}(\mathbf{R}_{\mathbf{H}} + \sigma_e^2 \mathbf{I}_{N_{\text{car}}})^{-1} \tilde{\mathbf{H}}(t), \quad (35)$$

and

$$\mathbf{C}_{\mathbf{H}|\text{CSI}} = \mathbf{R}_{\mathbf{H}} - \mathbf{R}_{\mathbf{H}}(\mathbf{R}_{\mathbf{H}} + \sigma_e^2 \mathbf{I}_{N_{\text{car}}})^{-1} \mathbf{R}_{\mathbf{H}}. \quad (36)$$

Note that in the case of perfect estimation (i.e.,  $\sigma_e^2 = 0$ ) we obtain perfect CSI, as (34), (35) and (36) reduce to  $\tilde{\mathbf{H}}(t) = \mathbf{H}(t)$ ,  $\mu_{\mathbf{H}|\text{CSI}} = \mathbf{H}(t)$  and  $\mathbf{C}_{\mathbf{H}|\text{CSI}} = 0$ .

#### Delayed CSI

Now we assume that the CSI is outdated, because of a delay in the feedback to the transmitter. At time instance  $t$ , the delayed CSI available at the transmitter is denoted by  $\mathbf{H}(t - \tau_d)$ , where  $\tau_d$  denotes the delay. In this case, it can be shown that

$$\mu_{\mathbf{H}|\text{CSI}} = J_0(2\pi f_d \tau_d) \mathbf{H}(t - \tau_d), \quad (37)$$

and

$$\mathbf{C}_{\mathbf{H}|\text{CSI}} = \left(1 - J_0(2\pi f_d \tau_d)^2\right) \mathbf{R}_{\mathbf{H}}. \quad (38)$$

When  $\tau_d = 0$ , we obtain perfect CSI, as (37) and (38) reduce to  $\mu_{\mathbf{H}|\text{CSI}} = \mathbf{H}(t)$  and  $\mathbf{C}_{\mathbf{H}|\text{CSI}} = 0$ .

#### Estimated and delayed CSI

In this section we assume that the CSI available at the transmitter is both delayed and estimated. We also consider the possibility that the transmitter has access to multiple delayed estimates. With  $P$  denoting the number of available estimates, the CSI which is available at the transmitter is given by

$$\text{CSI} = \left[ \tilde{\mathbf{H}}(t - \tau_d)^T \dots \tilde{\mathbf{H}}(t - P\tau_d)^T \right]^T, \quad (39)$$

where  $\tilde{\mathbf{H}}(t - k\tau_d)$  ( $\forall k \in \{1, \dots, P\}$ ) is defined as in (34). Defining the matrices

$$\mathbf{X} \triangleq [J_0(2\pi f_d \tau_d), J_0(2\pi 2f_d \tau_d), \dots, J_0(2\pi P f_d \tau_d)] \otimes \mathbf{R}_{\mathbf{H}}, \quad (40)$$

$$\mathbf{Y} \triangleq \mathbf{J} \otimes \mathbf{R}_{\mathbf{H}} + \mathbf{I}_P \otimes \sigma^2 \mathbf{I}_{N_{\text{car}}}, \quad (41)$$

where  $\mathbf{J} \in \mathbb{C}^{P \times P}$  with entries  $\mathbf{J}_{k,l} \triangleq J_0(2\pi f_d \tau_d(k-l))$ ,  $k = 1, \dots, P$ ;  $l = 1, \dots, P$ , and  $\otimes$  indicates the Kronecker product, it can be shown that

$$\mu_{\mathbf{H}|\text{CSI}} = \mathbf{X}\mathbf{Y}^{-1}\text{CSI}, \quad (42)$$

and

$$\mathbf{C}_{\mathbf{H}|\text{CSI}} = \mathbf{R}_{\mathbf{H}} - \mathbf{X}\mathbf{Y}^{-1}\mathbf{X}^H. \quad (43)$$

#### Acknowledgements

J. Van Hecke is supported by a Ph.D. fellowship of the Research Foundation Flanders (FWO).

This work was supported by the European Commission in the framework of the FP7 Network of Excellence in Wireless COMMunications NEWCOM# (Grant agreement no. 318306), and the Interuniversity Attraction Poles Programme initiated by the Belgian Science Policy Office.

#### Competing interests

The authors declare that they have no competing interests.

#### Author details

<sup>1</sup>Ghent University, Department of Telecommunications and Information Processing, 9000 Ghent, Belgium. <sup>2</sup>University of Pisa, Department of Information Engineering, I-56122 Pisa, Italy. <sup>3</sup>Université Catholique de Louvain, Institute of Information and Communication Technologies, Electronics and Applied Mathematics (ICTEAM), 1348 Louvain-la-Neuve, Belgium.

Received: 23 March 2016 Accepted: 20 September 2016

Published online: 26 October 2016

#### References

1. G Caire, G Taricco, E Biglieri, Bit-interleaved coded modulation. *Inf. Theory IEEE Trans.* **44**(3), 927–946 (1998). doi:10.1109/18.669123
2. AJ Goldsmith, S-G Chua, Variable-rate variable-power MQAM for fading channels. *Commun. IEEE Trans.* **45**(10), 1218–1230 (1997). doi:10.1109/26.634685
3. S Haykin, Cognitive radio: brain-empowered wireless communications. *Selected Areas Commun. IEEE J.* **23**(2), 201–220 (2005). doi:10.1109/JSAC.2004.839380

4. A Goldsmith, SA Jafar, I Maric, S Srinivasa, Breaking spectrum gridlock with cognitive radios: an information theoretic perspective. *Proc. IEEE*. **97**(5), 894–914 (2009). doi:10.1109/JPROC.2009.2015717
5. S Ye, RS Blum, LJ Cimini, Adaptive OFDM systems with imperfect channel state information. *Wireless Commun. IEEE Trans.* **5**(11), 3255–3265 (2006). doi:10.1109/TWC.2006.05004
6. A Kuhne, A Klein, Throughput analysis of multi-user OFDMA-systems using imperfect CQI feedback and diversity techniques. *Selected Areas Commun. IEEE J.* **26**(8), 1440–1450 (2008). doi:10.1109/JSAC.2008.081010
7. N Mokari, S Parsaeefard, P Azmi, H Saeedi, E Hossain, Robust ergodic uplink resource allocation in underlay OFDMA cognitive radio networks. *IEEE Trans. Mobile Comput.* **15**(2), 419–431 (2016). doi:10.1109/TMC.2015.2413782
8. D Tian, J Zhou, Z Sheng, VCM Leung, Robust energy-efficient MIMO transmission for cognitive vehicular networks. *IEEE Trans. Veh. Technol.* **65**(6), 3845–3859 (2016). doi:10.1109/TVT.2016.2567062
9. W Jaafar, T Ohtsuki, W Ajib, D Haccoun, Impact of the CSI on the performance of cognitive relay networks with partial relay selection. *IEEE Trans. Veh. Technol.* **65**(2), 673–684 (2016). doi:10.1109/TVT.2015.2402193
10. S Mallick, R Devarajan, RA Loodaricheh, VK Bhargava, Robust resource optimization for cooperative cognitive radio networks with imperfect CSI. *IEEE Trans. Wireless Commun.* **14**(2), 907–920 (2015). doi:10.1109/TWC.2014.2362135
11. S Singh, PD Teal, PA Dmochowski, AJ Coulson, Robust cognitive radio cooperative beamforming. *IEEE Trans. Wireless Commun.* **13**(11), 6370–6381 (2014). doi:10.1109/TWC.2014.2331074
12. H Huang, Z Li, J Si, L Guan, Underlay cognitive relay networks with imperfect channel state information and multiple primary receivers. *IET Commun.* **9**(4), 460–467 (2015). doi:10.1049/iet-com.2014.0429
13. S Nanda, KM Rege, Frame error rates for convolutional codes on fading channels and the concept of effective  $E_b/N_0$ . *Veh. Technol. IEEE Trans.* **47**(4), 1245–1250 (1998). doi:10.1109/25.728513
14. I Stupia, V Lottici, F Giannetti, L Vandendorpe, Link resource adaptation for multiantenna bit-interleaved coded multicarrier systems. *Signal Process. IEEE Trans.* **60**(7), 3644–3656 (2012). doi:10.1109/TSP.2012.2192110
15. E Tuomaala, H Wang, in *Mobile Technology, Applications and Systems, 2005 2nd International Conference On*. Effective SINR approach of link to system mapping in OFDM/multi-carrier mobile network (IEEE, New Jersey, 2005), pp. 5–5. doi:10.1109/MTAS.2005.243791
16. J Francis, NB Mehta, Characterizing the impact of feedback delays on wideband rate adaptation. *Wireless Commun. IEEE Trans.* **14**(2), 960–971 (2015). doi:10.1109/TWC.2014.2363083
17. TL Jensen, S Kant, J Wehinger, BH Fleury, Fast link adaptation for MIMO OFDM. *Veh. Technol. IEEE Trans.* **59**(8), 3766–3778 (2010). doi:10.1109/TVT.2010.2053727
18. D Qiao, S Choi, KG Shin, Goodput analysis and link adaptation for IEEE 802.11a wireless LANs. *IEEE Trans. Mobile Comput.* **1**(4), 278–292 (2002). doi:10.1109/TMC.2002.1175541
19. PD Fiorentino, R Andreotti, V Lottici, F Giannetti, JV Hecke, M Moeneclaey, in *European Wireless 2014; 20th European Wireless Conference; Proceedings Of*. Link resource adaptation for BIC-OFDM systems with outdated channel state information (VDE VERLAG, Berlin, 2014), pp. 1–6
20. J Van Hecke, P Del Fiorentino, R Andreotti, V Lottici, F Giannetti, L Vandendorpe, M Moeneclaey, in *Communications (ICC), 2015 IEEE International Conference On*. Goodput-maximizing resource allocation in cognitive radio BIC-OFDM systems with DF relay selection (IEEE, New Jersey, 2015), pp. 1404–1409. doi:10.1109/ICC.2015.7248520
21. J Van Hecke, P Del Fiorentino, R Andreotti, V Lottici, F Giannetti, L Vandendorpe, M Moeneclaey, in *Communications and Vehicular Technology in the Benelux (SCVT), 2015 IEEE 22st Symposium On*. Accurate modeling of the predicted kesm-based link performance metric for BIC-OFDM systems (IEEE, New Jersey, 2015)
22. A Ghasemi, ES Sousa, Fundamental limits of spectrum-sharing in fading environments. *Wireless Commun. IEEE Trans.* **6**(2), 649–658 (2007). doi:10.1109/TWC.2007.05447
23. UL Wijewardhana, M Codreanu, M Latva-aho, A Ephremides, A robust beamformer design for underlay cognitive radio networks using worst case optimization. *EURASIP J. Wireless Commun. Netw.* **2014**(1), 1–16 (2014). doi:10.1186/1687-1499-2014-37
24. E Björnson, E Jorswieck, *Optimal Resource Allocation in Coordinated Multi-Cell Systems*, vol. 9. (Foundations and Trends in Communications and Information Theory, Boston, 2013)
25. X Zhang, J Xing, Z Yan, Y Gao, W Wang, Outage performance study of cognitive relay networks with imperfect channel knowledge. *IEEE Commun. Lett.* **17**(1), 27–30 (2013). doi:10.1109/LCOMM.2012.112812.121371
26. K Ho-Van, PC Sofotasios, S Freear, Underlay cooperative cognitive networks with imperfect nakagami-m fading channel information and strict transmit power constraint: Interference statistics and outage probability analysis. *J. Commun. Netw.* **16**(1), 10–17 (2014). doi:10.1109/JCN.2014.000004
27. I Stupia, F Giannetti, V Lottici, R Andreotti, L Vandendorpe, AN D'Andrea, in *Future Network and Mobile Summit, 2010*. A greedy algorithm for goodput-oriented AMC in turbo-coded OFDM (International information management corporation (IIMC), Dublin, 2010), pp. 1–8
28. S Boyd, L Vandenberghe, *Convex optimization*. (Cambridge University Press, Cambridge, UK, 2004)
29. M Grant, S Boyd, CVX: Matlab Software for Disciplined Convex Programming, version 2.1 (2014). <http://cvxr.com/cvx>
30. I Stupia, F Giannetti, V Lottici, L Vandendorpe, in *Wireless Conference (EW), 2010 European*. A greedy algorithm for goodput-based adaptive modulation and coding in BIC-OFDM systems (IEEE, New Jersey, 2010), pp. 608–615. doi:10.1109/EW.2010.5483466
31. PL Nuaymi, *WiMAX: Technology for Broadband Wireless Access*. (John Wiley & Sons, New York, 2007). <https://books.google.co.uk/books?id=Kv5bdM9QIYC>
32. ETSI, Selection procedures for the choice of radio transmission technologies of the UMTS (UMTS 30.03 version 3.1.0). Technical report, UMTS. <http://www.etsi.org/>
33. WC Jakes, *Microwave Mobile Communications*. (John Wiley & Sons, New York, 1974)

Submit your manuscript to a SpringerOpen<sup>®</sup> journal and benefit from:

- Convenient online submission
- Rigorous peer review
- Immediate publication on acceptance
- Open access: articles freely available online
- High visibility within the field
- Retaining the copyright to your article

---

Submit your next manuscript at ► [springeropen.com](http://springeropen.com)